European Journal of Chemistry

View Journal Online
View Article Online

# Synthesis, analysis of single crystal structure and computational studies on a novel picrate derivative: 2-(Pyridine-2-ylthio)pyridine-1-ium picrate

Fatma Aydin [1,*] and Asli Ozturk Kiraz [2]

[1] *Department of Chemistry, Faculty of Science, Çanakkale Onsekiz Mart University, 17100, Çanakkale, Turkey*
[2] *Department of Physics, Computational Physics Laboratory, Faculty of Science, Pamukkale University, 20070, Denizli, Turkey*

* *Corresponding author at: Department of Chemistry, Faculty of Science, Çanakkale Onsekiz Mart University, 17100, Çanakkale, Turkey.*
*e-mail: faydin@comu.edu.tr (F. Aydin).*

RESEARCH ARTICLE

10.5155/eurjchem.16.2.117-128.2673

Received: 12 February 2025
Received in revised form: 18 April 2025
Accepted: 1 May 2025
Published online: 30 June 2025
Printed: 30 June 2025

KEYWORDS

Thermal properties
2-Mercaptopyridine
Density functional theory
X-ray structure determination
Molecular electrostatic potentials
2-(Pyridine-2-ylthio)pyridine-1-ium picrate

ABSTRACT

A new organic salt, 2-(pyridine-2-ylthio)pyridine-1-ium picrate ($C_{16}H_{11}N_5O_7S$: 2-PyrTPPc), has been synthesized and characterized using various spectroscopic methods such as $^1$H NMR, $^{13}$C NMR, and FT-IR. The crystal structure of the title compound was analyzed using X-ray structure analysis, which revealed that it belongs to the monoclinic $P2_1/c$ space group with $a$ = 16.876(4) Å, $b$ = 7.6675(18) Å, $c$ = 13.846(3) Å, $Z$ = 4, and $V$ = 1766.9(7) Å$^3$. The molecular packing of the compound showed the presence of several intermolecular hydrogen bonds between different atoms. The electronic properties of the crystal were investigated using density functional theory (DFT) with B3LYP/6-311G(d,p) level. Frontier molecular orbitals were drawn and related global quantities such as electronic chemical potential, chemical hardness-softness, electrophilicity, HOMO and LUMO energy eigenvalues, and the difference between HOMO and LUMO ($\Delta E$) were calculated and discussed. TG/DTG analysis revealed the thermal stability of the 2-PyrTPPc crystal. The single stage of decomposition and the sharpness of the peak in the temperature range of 157-224 °C illustrated the purity and good crystallinity of the grown crystal. The different vibration modes of the 2-PyrTPPc molecule were determined by analyzing the FT-IR and FT-Raman spectra. The detection of vibrations of the pyrNH$^+$ and aromatic thioether moiety supports the confirmation of the di(pyridin-2-yl)sulfane structure through the intermediate formed by the transfer of the proton from picric acid to 2-mercaptopyridine.

**Cite this**: *Eur. J. Chem.* **2025**, *16(2)*, 117-128 **Journal website**: www.eurjchem.com

## 1. Introduction

2-Mercaptopyridine is an organic sulfur compound that contains a mercapto(-SH) group in the *ortho* position of a pyridine ring. Due to its tautomerization reaction, the compound can exist in two forms: thione and thiol isomers [1,2]. 2-Mercaptopyridine is a Lewis base due to its base centers, such as pyridine and thiophenol. Both pyridine (p$K_a$ = 5.2) and thiophenol (p$K_a$ = 6.0) have Lewis base properties, but the thiophenol unit is more basic. Thiophenol can be used as a reagent for unsymmetrical disulfide derivatives [3], alkylating agents [4], and chelating ligands [5]. It can also be used as a selective glutathione (GSH) detection reagent [6]. With this powerful reducing agent, you can selectively oxidize it to 2,2'-(dipyridyl)disulfide [7].

Picric acid is an organic acid derived from phenol and contains three nitro groups. Due to its stabilization of the phenolate anion through the resonance of nitro groups, picric acid has become one of the strongest organic acids (p$K_a$ = 0.42). Picric acid, which is an electron acceptor, can form charge transfer complexes or ammonium salts with various aliphatic amines [8] and aromatic amines such as some aniline derivatives [9,10] and pyridine derivatives [11-13]. It is also known for its ability to form π-π* interactions with aromatic hydrocarbons [14,15]. Picric acid forms simple picrate salts from dimeric cations of the AA+ type, where A and A+ are amino acids in the Zwitter ionic and singly charged cationic states [16-18]. Many molecular organic change transfer crystals of picric acid(donor) with organic acceptor molecules exhibit especially applications such as organic non-linear optical material (NLO) [19,20]. The purpose of this comment is to point out that the title of the article is 2-(pyridine-2-ylthio)pyridine-1-ium picrate ($C_{10}H_8N_2S{\cdot}C_6H_3N_3O_7$) and not 2-mercaptopyridinium picrate ($C_5H_5NS{\cdot}C_6H_3N_3O_7$) as might appear when reading the article. Pyridine is an analog of benzene and can undergo an aromatic nucleophilic substitution reaction, similar to benzene, through an E1cB alkyne elimination reaction mechanism [21,22].

In this study, we successfully synthesized a novel picrate salt using a distinctive synthetic pathway, as illustrated in Scheme 1. The structure of the compound was thoroughly characterized through elemental analysis and a variety of spectroscopic techniques, including FT-IR, $^1$H NMR, and $^{13}$C NMR. The crystal structure was determined via single-crystal X-ray diffraction. To explore the electronic properties, global reactivity, thermal properties, and NBO analysis of the compound, we performed density functional theory (DFT) calculations at the B3LYP/6-311G(d,p) level.


ISSN 2153-2249 (Print) / ISSN 2153-2257 (Online) 
https://dx.doi.org/10.5155/eurjchem.16.2.117-128.2673

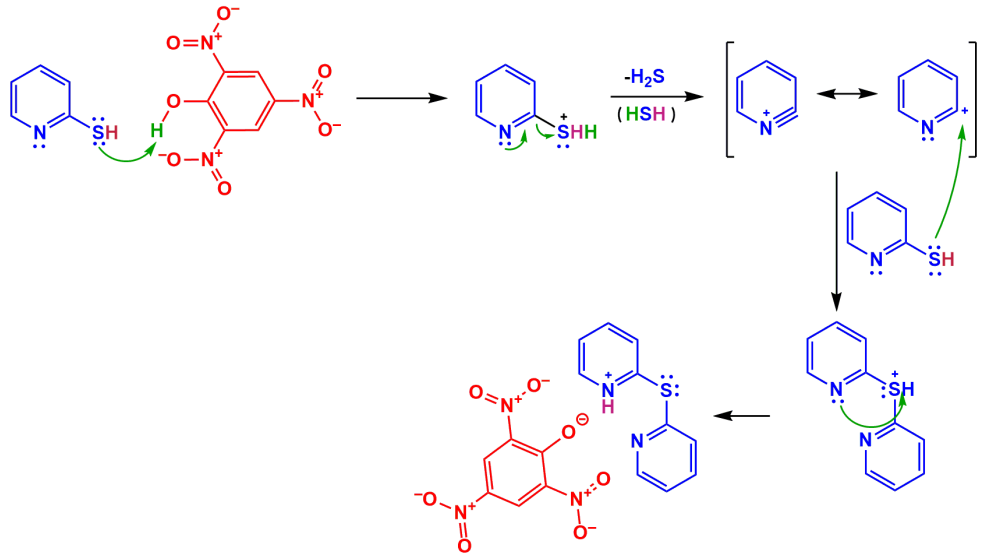


**Scheme 1**. Reaction pathway for the synthesis of the title compound, 2-PyrTPPc.

**Figure 1.** Photograph of the 2-PyrTPPc crystals.

The exceptional features of both experimental and theoretical infrared and Raman spectra were meticulously examined in the article [23,24].

## 2. Experimental

### *2.1. General remarks*

2,4,6-Trinitrophenol (picric acid), 2-mercaptopyridine, ethanol, tetrahydrofuran, and chloroform were purchased from Sigma-Aldrich and Merck Chemicals. The melting point of the compound was determined using an Electrothermal 9100® apparatus. Elemental analyzes were carried out using a Carlo-Erba instrument. FT-IR analysis was performed on a Perkin Elmer Spectrum-100 FT-IR instrument with an ATR apparatus in the range of 4000-650 $cm^{-1}$. The Raman spectrum was recorded in the region of 3500-150 $cm^{-1}$ on a WITEC ALPHA 300RA FT-Raman spectrometer using a 532 nm green laser. The $^{1}H$ NMR and $^{13}C$ NMR spectra were recorded on a Bruker GmbH NMR spectrometer using $CDCl_3$ as a solvent and TMS as the internal standard. Crystal structure analysis of the compound was performed using a Bruker D8 QUEST X-ray diffractometer (MoKα radiation, λ = 0.71073). TG/DTG analysis of the compound was performed using a Perkin Elmer TGA8000 instrument. Thermogravimetric analysis (TGA) of the sample (8.899 mg) was carried out under a nitrogen atmosphere with a heating rate of 20 °C/min from 30 to 800 °C on a PerkinElmer TGA 8000 analyzer.

### *2.2. Synthesis of 2-(pyridine-2-ylthio)pyridine-1-ium picrate, 2-PyrTPPc*

Commercial picric acid (1% in $H_2O$) purchased from Sigma-Aldrich was crystallized using ethanol. The resulting crystallized picric acid (2.29 g, 10 mmol) was dissolved in chloroform (20 mL), and 2-mercapto pyridine (1.11 g, 10 mmol) in chloroform (15 mL) was added dropwise to the solution. The mixture was refluxed with stirring for four hours. After that, the reddish oil product obtained was crystallized by slow evaporation of chloroform. The reddish seed crystal of the title compound was grown by the slow evaporation method, after dissolving the crystallized salt in THF at room temperature. After 20 days, a good quality single crystal was harvested and is shown photographically in Figure 1. 2-(Pyridine-2-ylthio)pyridine-1-ium picrate (2-PyrTPPc): Color: Reddish. Yield: 78%. M.p.: 157-158 °C. FT-IR (ν, $cm^{-1}$): 3472, 3442, 3369, 3214, 3097, 1636, 1598, 1564, 1471, 1422, 1385, 1334, 1316, 1246, 1153, 1071, 1067, 981, 928, 908, 823, 772, 701. $^{1}H$ NMR (400 MHz, $CDCl_3$, δ, ppm): 14.07 (brs, 1H, $NH^+$), 7.71, 7.70, 7.68, 7.59, 7.46, 7.44, 7.42, 7.33, 6.86, 6.84 (10 H, Ar-H). $^{13}C$ NMR (100 MHz, $CDCl_3$, δ, ppm): 176.45 (NH=C-S), 156.10 (C-$O_{phenoxy}$), 149.33 (N=C-S), 137.87, 126.10, 122.18 ($C_{phenoxy}$), 137.76, 133.20, 119.93, 114.56 ($C_{prydinyl}$). Anal. calcd. for $C_{16}H_{11}N_5O_7S$: C, 46.05; H, 2.66; N, 16.78; S, 7.68; Found: C, 46.12; H, 2.70; N, 16.69; S, 7.65%.

### *2.3. X-ray crystallography*

X-ray diffraction data for a single crystal were collected using MoKα radiation at a wavelength of 0.71073 Å at a temperature of 273(2) K. The structure was determined using SHELXS-97 and refined using SHELXL-97 least squares on $F^2$ [25]. Absorption correction was performed using the multi-scan method. These data are available free of charge from the Cambridge Crystallographic Data Center at www.ccdc.cam.ac.uk/data_request/cif.

**Table 1.** Crystal data, data collection, and refinement parameters for the title compound, 2-PyrTPPc.

| | |
|---|---|
| Empirical formula | $C_{16}H_{11}N_5O_7S$ |
| Formula weight (g/mol) | 417.36 |
| Temperature (K) | 273(2) |
| Crystal system | Monoclinic |
| Space group | $P2_1/c$ |
| *a* (Å) | 16.876(4) |
| *b* (Å) | 7.6675(18) |
| c (Å) | 13.846(3) |
| α (°) | 90 |
| β (°) | 99.543(7) |
| γ (°) | 90 |
| Volume (Å$^3$) | 1766.9(7) |
| *Z* | 4 |
| $\rho_{calc}$ (g/cm$^3$) | 1.569 |
| μ (mm$^{-1}$) | 0.237 |
| F (000) | 856.0 |
| Crystal size (mm$^3$) | 0.4 × 0.27 × 0.18 |
| Radiation | MoKα (λ = 0.71073) |
| 2Θ range for data collection (°) | 2.4 to 53.48 |
| Index ranges | $-21 \le h \le 21$, $-9 \le k \le 9$, $-17 \le l \le 17$ |
| Reflections collected | 30487 |
| Independent reflections | 3741 [$R_{int}$ = 0.0387, $R_{sigma}$ = 0.0313] |
| Data/restraints/parameters | 3741/0/306 |
| Goodness-of-fit on F$^2$ | 1.018 |
| Final R indexes [I≥2σ(I)] | $R_1$ = 0.0469, $wR_2$ = 0.1039 |
| Final R indexes [all data] | $R_1$ = 0.0768, $wR_2$ = 0.1221 |
| Largest diff. peak/hole (e.Å$^{-3}$) | 0.33/-0.28 |
| Measurement | Bruker Kappa APEXII CCD |
| Programs system | SHELXTL-97 |
| Structure determination | SHELXS-97 |
| CCDC deposition number | 2335699 |

### *2.4. Computational studies*

Quantum chemical calculations were carried out in the neutral ground state of the title compound (charge: 0, multiplicity: 1) using Gaussian16 [26] and GaussView 6.0 [27]. The Gaussian package is a tool that uses model chemistry to determine the shapes and energies of orbitals in a given molecule. However, density functional theory (DFT) methods describe the interaction between electrons and the total electron density. The most commonly used DFT method is the Becke3 parameter, which calculates the molecular energy for overlapping orbitals. Basis sets are used to increase the number of basis functions per atom. The split-valence triple-zeta basis set 6-311G(d,p) is a popular choice because it allows orbitals to change size but not shape. This basis set has various origins and is recommended by Foresman and Frisch for atoms in the periodic table from hydrogen to bromine [28]. For modeling, the initial guess of picrate was obtained first from the X-ray coordinates and transformed into the Z-matrix format with the Babel program [29]; the model starting geometry of picrate was obtained and applying ab initio optimization at B3LYP/6-311G(d,p) level.

## 3. Results and discussion

### *3.1. Synthesis*

Aliphatic and aromatic amine picrate complexes are generally formed from the interactions of various amine compounds with picric acid. However, due to the difference in Lewis basic properties of thiols and amines, the proton transfer region in picrate complexes changes. In our study using the 2-mercaptopyridine compound, it was observed that it was not 2-mercaptopyridinium picrate ($C_5H_5NS{\cdot}C_6H_3N_3O_7$) but 2-(pyridin-2-ylthio)pyridin-1-ium picrate,($C_{10}H_8N_2S{\cdot}C_6H_3N_3O_7$) was formed via a different mechanism due to the structure and region of the proton transfer center. The C-H protons, which are consistent with the protons of the pyridinium ring, resonate around δ 6.84-7.71 ppm from TMS. The N-H protons of the pyridinium salt are responsible for the broad signal observed at δ 14.07 ppm from TMS [30]. The ipso carbon (C19) of the picrate moiety is responsible for the faint carbon signal at δ 176.45 ppm. The aromatic carbons (C21 and C24) of the pyridinium group bonded to the sulfur atom appear at δ 156.10 ppm. At δ 137.87 ppm, the aromatic carbon atoms C17 and C18 of the same type appear in the picrate moiety. The carbon atoms C15, C16, C14 and C20-C29 in the other aromatic moieties of the complex were assigned to the peak that appeared at δ 149.93, 137.76, 133.20, 126.30, 122.18, 116.93, and 114.56 ppm, respectively.

### *3.2. Crystal structure and optimized geometry*

The crystal structure of 2-(pyridine-2-ylthio)-pyridine-1-ium picrate is monoclinic with the space group $P2_1/c$ with $Z = 4$ in the unit cell. The asymmetric unit contains one pyridinium and one picrate ion. Due to the functional groups of the title compound, the *b*-axis and the *c*-axis (7.6675(18) and 13.846(3) Å, respectively) are larger than the *a*-axis (16.876(4) Å) in the crystal dimensions. All non-hydrogen atoms were refined anisotropically; all other hydrogen atoms were calculated to their idealized positions and a riding model was used. Information on the crystal data, experimental conditions and structural refinement can be found in Table 1.

The ORTEP view of the molecular structure of the picrate crystal is shown in Figure 2. Furthermore, the optimized geometric structure of the title compound obtained from the DFT/B3LYP/6-311G(d,p) method is shown in Figure 3 with the atom numbering scheme.

Table 2 shows the final positional parameters of the title compound. The molecule is composed of six-membered two rings of pyridine and one benzene ring. In the six-membered pyridine rings C20/C23/C29/C28/C24/N12 and C21/C22/C26/C27/C25/N7 are planers having total puckering amplitudes $Q_T$ of 0.0124(3) Å [$\varphi_2$ = -120.67(13.01)°, $\theta_2$ = 108.51(11.17)°] and 0.0099(3) [$\varphi_2$ = -63.49(17.23)°, $\theta_2$ = 85.31(16.39)°], respectively. Also, the six-membered benzene ring C14/C15/C18/C19/C17/C16 is almost coplanar with the parameters $Q_T$ = 0.0497(3) Å, [$\varphi_2$ = 98.65(2.64)°, $\theta_2$ = 92.44(2.72)° [31].

The bond lengths, bond angles and dihedral angles are obtained from the geometry optimization which used starting geometries taken from the X-ray structure determination.

**Table 2.** Selected experimental and optimized structural parameters of the title compound, 2-PyrTPPc.

| Parameters | B3LYP/6-311G(d,p) | Exp. (Present work) | Parameter | B3LYP/ 6-311G(d,p) | Exp. (Present work) |
|---|---|---|---|---|---|
| *Bond lengths (Å)* | | | | | |
| S1-C21 | 1.768 | 1.749(3) | N9-O13 | 1.235 | 1.220(3) |
| S1-C24 | 1.793 | 1.779(3) | N9-O10 | 1.227 | 1.229(3) |
| O2-N5 | 1.229 | 1.233(2) | N9-C18 | 1.457 | 1.456(3) |
| O3-N5 | 1.230 | 1.231(2) | N12-C24 | 1.334 | 1.337(3) |
| O4-N8 | 1.227 | 1.225(3) | N12-C20 | 1.343 | 1.347(3) |
| N5-C14 | 1.453 | 1.447(3) | C14-C15 | 1.392 | 1.382(3) |
| N7-C21 | 1.351 | 1.342(3) | C14-C16 | 1.396 | 1.389(3) |
| N7-C25 | 1.354 | 1.346(3) | C15-C18 | 1.378 | 1.370(3) |
| N8-O11 | 1.231 | 1.218(2) | C16-C17 | 1.375 | 1.361(3) |
| N8-C17 | 1.461 | 1.463(3) | C17-C19 | 1.466 | 1.453(3) |
| *Bond angles (°)* | | | | | |
| O2-N5-C14 | 117.88 | 118.20(19) | N9-C18-C19 | 119.90 | 119.42(19) |
| O3-N5-O2 | 124.19 | 123.39(19) | O10-N9-C18 | 118.44 | 118.6(2) |
| O3-N5-C14 | 117.93 | 118.40(19) | O11-N8-O4 | 123.45 | 122.6(2) |
| O4-N8-C17 | 118.03 | 118.64(19) | O11-N8-C17 | 118.48 | 118.6(2) |
| O6-C19-C17 | 123.72 | 123.8(2) | N12-C20-C23 | 122.91 | 123.1(3) |
| O6-C19-C18 | 124.35 | 125.5(2) | N12-C24-C28 | 122.79 | 123.1(2) |
| N7-C21-C22 | 119.59 | 118.1(3) | N12-C24-S1 | 122.06 | 120.39(19) |
| N7-C21-S1 | 122.70 | 122.25(19) | O13-N9-O10 | 122.99 | 122.4(2) |
| N7-C25-C27 | 120.18 | 120.3(3) | O13-N9-C18 | 118.53 | 119.0(2) |
| C15-C14-N5 | 119.58 | 120.00(19) | C15-C14-C16 | 120.78 | 120.77(19) |
| C15-C18-N9 | 116.52 | 116.4(2) | C16-C17-N8 | 116.76 | 115.9(2) |
| C15-C18-C19 | 123.57 | 124.2(2) | C16-C17-C19 | 123.83 | 125.4(2) |
| C16-C14-N5 | 119.61 | 119.23(19) | C17-C16-C14 | 119.65 | 119.0(2) |
| C15-C14-N5 | 119.58 | 120.00(19) | C17-C19-C18 | 111.85 | 110.70(18) |
| C16-C17-N8 | 116.76 | 115.9(2) | C18-C15-C14 | 119.79 | 119.7(2) |
| C21-S1-C24 | 107.04 | 107.63(11) | C19-C17-N8 | 119.41 | 118.70(18) |
| C21-N7-C25 | 122.30 | 122.3(2) | C22-C21-S1 | 117.70 | 119.6(2) |
| C24-N12-C20 | 118.48 | 117.6(2) | C28-C24-S1 | 115.15 | 116.5(2) |
| *Dihedral angles (°)* | | | | | |
| S1-C21-C22-C26 | 177.99 | 179.0(2) | O11-N8-C17-C16 | 149.77 | 137.8(2) |
| S1-C24 -C28-C29 | -179.30 | 177.7(2) | O11-N8-C17-C19 | -31.06 | 42.4(3) |
| O2-N5-C14-C15 | 0.92 | 172.3(2) | N12-C20-C23-C29 | 0.12 | 1.5(4) |
| O2-N5-C14-C16 | 0.92 | 8.4(3) | N12-C24-C28-C29 | 0.02 | 0.6(4) |
| O3-N5-C14-C15 | -0.87 | 8.6(3) | O13-N9-C18-C15 | -152.32 | 154.0(2) |
| O3-N5-C14-C16 | -179.12 | 170.7(2) | O13-N9-C18-C19 | 28.51 | 26.6(3) |
| O4-N8-C17-C16 | -28.06 | 38.4(3) | C14-C15-C18-N9 | 176.67 | 175.99(19) |
| N5-C14-C15-C18 | -178.81 | 179.22(19) | C14-C15-C18-C19 | -4.19 | 4.7(3) |
| N5-C14-C16-C17 | 178.80 | 176.07(19) | C14-C16-C17-C19 | 4.23 | 5.2(3) |
| N7-C21-C22-C26 | -0.92 | 0.0(4) | C14-C16-C17-N8 | -176.64 | 174.94(19) |
| N7-C25-C27-C26 | -0.44 | 0.2(4) | C16-C17-C19-C18 | -8.06 | 2.3(3) |
| N8-C17-C19-O6 | -10.15 | 1.8(3) | C15-C14-C16-C17 | 0.57 | 3.2(3) |
| N8-C17-C19-C18 | 172.83 | 177.91(18) | C15-C18-C19-O6 | -168.97 | 176.9(2) |
| N9-C18-C19-O6 | 10.13 | 2.4(3) | C15-C18-C19-C17 | 8.03 | 2.8(3) . |
| N9-C18-C19-C17 | -172.87 | 177.88(19) | C16-C14-C15-C18 | -0.58 | 1.5(3) |
| O10-N9-C18-C15 | 25.52 | 25.0(3) | C20-N12-C24-C28 | 0.14 | 0.5(4) |
| O10-N9-C18-C19 | -153.64 | 154.4(2) | C20-N12-C24-S1 | 179.41 | 177.64(18) |
| C20-C23-C29-C28 | 0.05 | 1.4(4) | C22-C26-C27-C25 | -0.22 | 0.7(4) |
| C21-S1-C24-N12 | 3.62 | 5.2(2) | C24-S1-C21-N7 | -4.24 | 7.6(2) |
| C21-S1-C24-C28 | -177.05 | 173.05(19) | C24-S1-C21-C22 | 176.89 | 173.5(2) |
| C21-N7-C25-C27 | 0.42 | 1.0(4) | C24-N12-C20-C23 | -0.21 | 0.5(4) |
| C21-C22-C26-C27 | 0.89 | 0.8(4) | C24-C28-C29-C23 | -0.12 | 0.4(4) |
| C25-N7-C21-C22 | 0.28 | 0.9(4) | C25-N7-C21-S1 | -178.58 | 179.9(2) |

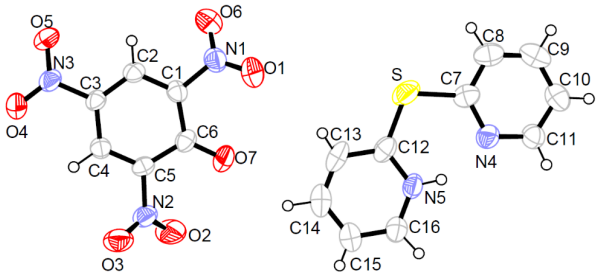


**Figure 2.** ORTEP III drawing of the title compound, 2-PyrTPPc with the atom-numbering scheme. Displacement ellipsoids are drawn at the 50% probability level [30].

To compare the theoretical results with the experimental one, some selected geometrical parameters are gathered in Table 2. The calculated S-C, N-C, and O-N bond lengths agree well with the experimental bond lengths, while the O4-N8, N8-C17, N9-O10 bond lenghts are nearly 0.002 Å and the N9-C18 bond length is nearly 0.001 Å longer. The calculated C-C and C=C bond lengths are also close to those from the X-ray data. The calculated O-N-C, O-C-C, N-C-S, N-C-C, O-N-O, C-C-S, C-S-C, and C-C-C bond angles are consistent with the experimental data except for the N12-C24-S1 bond angle. The theoretical value of this angle is slightly different from the experimental value, with the N12-C24-S1 bond angle being theoretically 122.06° and experimentally 120.39(19)°. This difference in angle is due to the limitations of the DFT method [32].

**Table 3.** Hydrogen bond between some atom (Å, °) for the compound, 2-PyrTPPc.

| D-H···A | D-H (Å) | D···A (Å) | H···A (Å) | D-H···A (°) |
|---|---|---|---|---|
| N7-H40···N12$^{i}$ | 0.85(3) | 2.630(3) | 1.85(3) | 150(3) |
| C16-H30···O2$^{ii}$ | 0.96(2) | 3.255(3) | 2.59(2) | 127.12(17) |
| C15-H31···O10$^{i}$ | 0.93(2) | 2.703(3) | 2.38(2) | 100.1(16) |
| C26-H32···O6$^{ii}$ | 0.98(3) | 3.128(4) | 2.36(3) | 135(2) |
| C25-H34···O6$^{iii}$ | 0.95(3) | 3.252(3) | 2.35(3) | 159(2) |
| C25-H34···O11$^{iii}$ | 0.95(3) | 3.097(3) | 2.41(3) | 128(2) |

Symmetry codes: (i) *x*, *y*, *z*; (ii) -*x*, 1-*y* ,1-*z*; (iii) *x*, 3/2-*y*, -1/2+*z*.

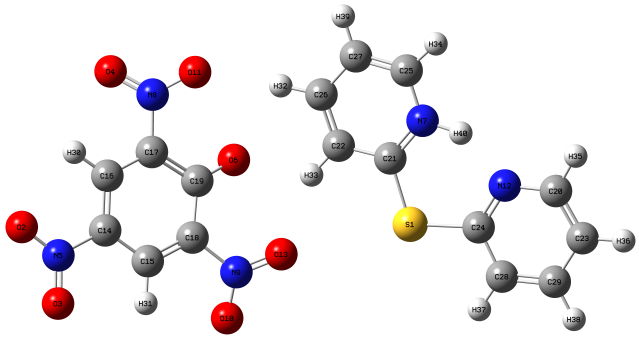

**Figure 3**. The ground state optimized geometry for the title compound, 2-PyrTPPc.

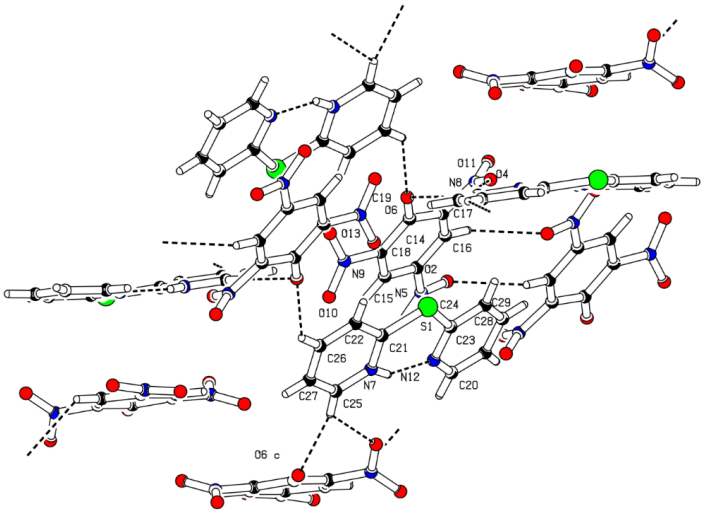


**Figure 4.** Intramolecular and intermolecular H-bonds in the dimer. The dotted lines represent C–H···O and N-H···N hydrogen interactions of the title compound, 2-PyrTPPc.

The crystal structure is an impressive display of molecular architecture, with inter- and intramolecular hydrogen bonding playing a crucial role. The arrangement of these bonds has been carefully planned to ensure optimal balance and stability within the structure. This systematic design provides a comprehensive overview of the structural dynamics involved. These balance and stability are also evident from the NBO analysis parameters. The stabilization energies between the donor S1(LP) and the acceptor C24-N12 bond were found to have a low value of 4.31 kcal/mol. The orientation of the pyridine and benzene rings is also defined by torsion angles.

The compound demonstrates intramolecular and intermolecular N-H···N and C-H···O hydrogen bonds in the crystal (Table 3). This type of C-H···X (X =O, N) hydrogen bond has been well reviewed in the literature [33]. The notable properties of the crystal arise from an intricately organized and balanced structural framework. This framework is formed through complex interactions that involve both intermolecular and intramolecular hydrogen bonding. Intermolecular hydrogen bonds occur between separate molecules, whereas intramolecular bonds form within a single molecule. The synergistic effects of these bonding interactions enhance not only the stability of the crystal but also the ability to significantly influence its various physical and chemical properties. A comprehensive analysis of these interactions and their implications is detailed in Table 3.

The title compound consists of dimeric units that are formed by hydrogen bonds between the C-H···O and N-H···N in the picrate rings. These dimeric units are then connected by paired C-H···O and N-H···N hydrogen bonds, forming sheets along the *a*-axis, as shown in Figure 4.

### *3.3. FT-IR and Raman spectral analysis*

FT-IR spectra confirm the presence of various functional groups and chemical bonds such as hydrogen bonds in the compounds. In the FT-IR spectrum, some functional groups have disappeared, while others have appeared due to picrate salts (Figure 5).

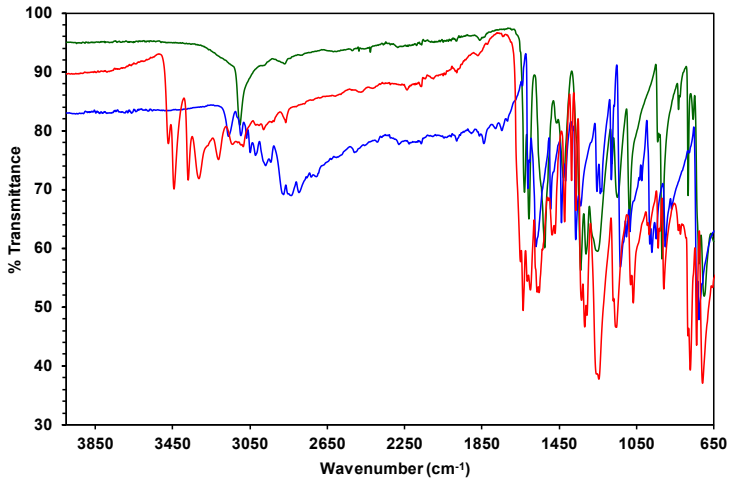


**Figure 5.** FT-IR spectrum of 2-(pyridine-2-ylthio)pyridine-1-ium picrate (2-PyrTPPc), 2-mercaptopyridine, 2,4,6-trinitrophenol (picric acid) (red, blue, and green line, respectively).

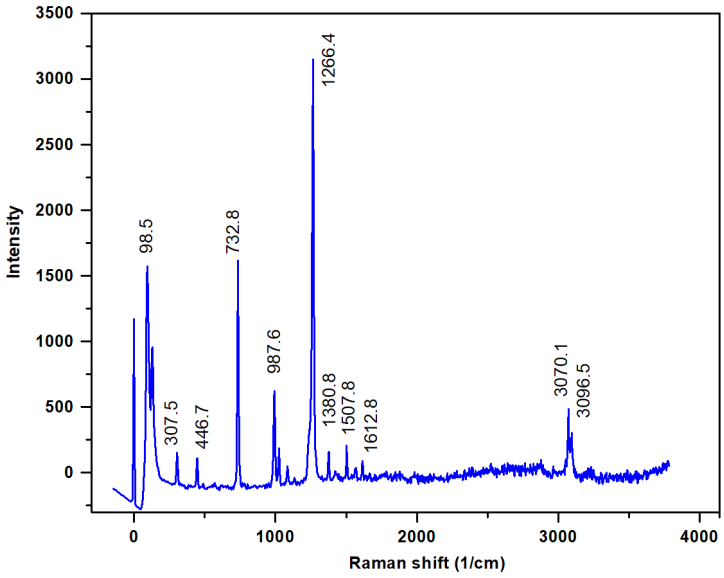


**Figure 6.** RAMAN spectrum of the title compound, 2-PyrTPPc.

The experimental characteristic FT-IR and Raman spectra along with the calculated (DFT, B3LYP method at 6-311G(d,p) level) in the gas-phase transmission spectra of the title compound are shown in Figures 5-7. The calculated wavenumbers corresponding to the normal modes of the FT-IR spectra are listed in Table 4.

Protonation of pyridine nitrogen to form the pyridinium salt gives rise to several bands from the $N^+$-H stretching between 3300 and 1950 $cm^{-1}$ that have moderate IR intensity, but are weak in the Raman spectrum. Due to the strong intermolecular hydrogen bond between the nitrogen atoms of the other pyridine, the characteristic peak of the $N^+$-H group was observed in the vibrational spectra of the pyridinium moiety at 3471 and 3443 $cm^{-1}$ [34].

In the Raman spectrum, these peaks do not appear very prominent (Figure 7). The C-H vibrations cover the asymmetric and symmetric stretching modes of two different pyridine rings in the phenolic group. Absorption above 3000 $cm^{-1}$(3369, 3314, and 3213 $cm^{-1}$) is attributed to the stretching vibrations of $\nu(C_{ring}\text{-}H)$ of the aromatic rings, such as pyridinium rings and phenolic rings [35]. The calculated infrared stretching vibrations of the C-H bond of the aromatic ring are around 2970-2880 $cm^{-1}$, whereas these peaks of the experimental spectrum appear around 3085-2999 and 3000 $cm^{-1}$, respectively [36]. In addition, the symmetric and asymmetric stretching vibrations of the C-S bond of the aromatic thioether moiety of the title compound, which are experimentally found at 771, 738, and 707 $cm^{-1}$, are attributed to the calculated peaks at 734, 712, and 486 $cm^{-1}$, respectively [37]. On the other hand, the asymmetric and symmetric stretching vibrations of the $NO_2$ group of the picrate anion are responsible for the sharp bands that appear experimentally at 1487-1422 $cm^{-1}$ in the FT-IR and at 1481 and 1446 $cm^{-1}$ in the calculated spectra [38]. The comparison between Raman and IR spectra of the vibrational modes in the title compound is more easily emphasized. Other characteristic peaks are observed at 987, 732 $cm^{-1}$ in the Raman spectra, which are caused by the out-of-plane bending(O-N=O) and scissoring (O-N=O) vibration modes of the nitro groups, respectively [39]. These assignments are very characteristic of the picrate anion. These assignments are very characteristic of picrate anions [40]. The experimental and the calculated vibrational frequencies agree well and confirm the formation of the structure of the title compound.

**Table 4.** Vibrational wavenumbers of the title compound, 2-PyrTPPc obtained from B3LYP/6-311G(d,p) in $cm^{-1}$, assignment with TED (total energy distribution).

| Modes | Unscaled | Scaled [a] | IR | Assignment [TED] [b] ≥ 10% |
|---|---|---|---|---|
| 1 | 9.898 | 9.570 | 0.816 | νCC(28%)+δCCN(15%) |
| 2 | 15.90 | 15.37 | 0.931 | νCC(21%)+δCCN(47%)+νON(16%) |
| 3 | 22.51 | 21.77 | 0.640 | νCC(16%)+δNCC(17%)+δCNC(11) |
| 4 | 30.96 | 29.94 | 0.111 | νNC(11%) |
| 5 | 38.59 | 37.32 | 2.793 | νCC(21%)+τHCCN(13%) |
| 6 | 54.16 | 52.37 | 5.390 | δCNC(12%) |
| 8 | 61.55 | 59.52 | 1.857 | νCC(19%) |
| 9 | 63.78 | 61.68 | 0.671 | νCH(20%) |
| 10 | 74.91 | 72.43 | 3.314 | νCH(10%)+νCC(13%)+δCCC(11%) |
| 11 | 95.56 | 92.41 | 3.257 | νCH(16%) |
| 12 | 107.5 | 104.0 | 6.585 | νCH(14%) |
| 13 | 135.1 | 130.6 | 6.337 | νCH(12%)+νCC(10%) |
| 14 | 147.0 | 142.2 | 28.17 | νNC(32%)+νSC(20%) |
| 15 | 156.2 | 151.0 | 1.578 | νCH(16%)+νCC(13%)+δNCC(16%) |
| 16 | 178.2 | 172.3 | 0.501 | νCC(14%)+δCCC(29%) |
| 17 | 183.0 | 176.9 | 0.378 | νCH(16%)+τCCOH(11%) |
| 19 | 198.1 | 191.5 | 0.017 | νNC(17%) |
| 20 | 262.3 | 253.6 | 5.084 | νCC(23%)+δCCC(33%) |
| 21 | 292.2 | 282.6 | 4.636 | νCC(20%)+τCNCC(13%)+τNCCC(11%)+γSCNC(15%) |
| 22 | 298.5 | 288.7 | 3.311 | νCH(13%)+δHCC(37%) |
| 23 | 308.3 | 298.1 | 1.567 | τCNCC(16%) |
| 24 | 328.6 | 317.7 | 2.192 | νCC(29%)+δCCC(14%) |
| 25 | 353.6 | 341.9 | 8.371 | νCC(20%)+γNCCC(12%) |
| 26 | 365.3 | 353.2 | 1.216 | νCC(72%) |
| 27 | 387.4 | 374.7 | 1.851 | τHCCC(13%) |
| 28 | 394.0 | 381.0 | 0.646 | τHCCC(30%) |
| 29 | 410.9 | 397.3 | 1.929 | δHCC(15%) |
| 30 | 455.8 | 440.8 | 4.056 | νCC(12%)+δHCC(33%) |
| 31 | 474.2 | 458.6 | 0.695 | νCH(43%)+δHCC(34%) |
| 32 | 478.3 | 462.5 | 9.969 | νCH(18%)+τHNCC(16%)+τ□CCC(16%) |
| 33 | 486.7 | 470.6 | 1.674 | νSC(31%) |
| 34 | 492.2 | 476.0 | 0.451 | νCH(12%)+τHCCC(11%) |
| 36 | 525.3 | 508.0 | 5.228 | νNH(10%)+δHCC(11%) |
| 37 | 552.3 | 534.0 | 4.109 | νCH(32%)+δHCC(19%) |
| 38 | 631.4 | 610.5 | 0.830 | τCCCN(16%) |
| 39 | 650.8 | 629.3 | 7.315 | νNH(11%)+δHNC(44%) |
| 40 | 689.0 | 666.25 | 12.71 | δCCC(16%)+τCCCC(30%)+τNCCC(10%) |
| 41 | 693.2 | 670.30 | 12.33 | νCC(11%)+γCNSC(12%) |
| 42 | 712.7 | 689.18 | 4.685 | γCSCC(12%) |
| 43 | 724.4 | 700.47 | 26.86 | νCC(11%) |
| 44 | 729.7 | 705.62 | 3.423 | δCCC(11%)+τCSCC(11%) |
| 45 | 734.2 | 709.92 | 69.77 | γSCNC(10%) |
| 46 | 737.8 | 713.42 | 28.24 | τONCC(13%)+τNCSC(11%) |
| 47 | 744.8 | 720.17 | 0.281 | νNC(13%) |
| 48 | 746.5 | 721.9 | 18.53 | νNC(17%) |
| 49 | 776.2 | 750. 6 | 80.03 | νNC(12%) |
| 50 | 780.9 | 755.2 | 0.681 | νONC(20%)+νCC(20%) |
| 54 | 848.8 | 820.8 | 0.218 | δCCC(10%) |
| 56 | 927.7 | 897.1 | 43.01 | νCC(24%)+δCCC(13%) |
| 57 | 942.2 | 911.1 | 9.093 | δCCC(10%) |
| 61 | 984.3 | 951.9 | 1.841 | δONC(17%) |
| 63 | 1011 | 977.3 | 7.917 | τONCC(20%) |
| 64 | 1021 | 987.1 | 0.151 | νON(14%) |
| 65 | 1022. | 988.2 | 15.64 | νON(46%)+δONO(10%) |
| 66 | 1051 | 1017 | 29.22 | δONC(31%) |
| 67 | 1056 | 1021 | 10.14 | τONCC(13%) |
| 68 | 1066 | 1031 | 7.753 | νOC(13%) |
| 69 | 1078 | 1042 | 1.680 | τONCC(47%)+γOCON(17%) |
| 70 | 1086 | 1051 | 105.7 | δONC(19%) |
| 71 | 1110 | 1073 | 24.81 | νON(11%) |
| 72 | 1120 | 1083 | 15.68 | δHCC(23%) |
| 73 | 1141 | 1103 | 55.57 | δONC(11%)+δNCC(18%) |
| 76 | 1177 | 1138 | 95.07 | νCC(12%) |
| 77 | 1186 | 1146 | 5.565 | γOCON(14%) |
| 78 | 1198 | 1158 | 20.47 | νON(16%) |
| 79 | 1268 | 1226 | 47.88 | νCC(23%) |
| 82 | 1310 | 1267 | 29.38 | γOCON(12%) |
| 84 | 1347 | 1302 | 4.089 | δ□COH(10%) |
| 85 | 1347 | 1303 | 658.7 | νNC(12%) |
| 86 | 1370 | 1325 | 67.27 | νON(12%) |
| 87 | 1390 | 1344 | 46.23 | νCC(13%) |
| 89 | 1451 | 1403 | 59.46 | νNC(21%) |
| 90 | 1468 | 1420 | 78.03 | γNCCC(10%) |
| 91 | 1479 | 1430 | 190.9 | νON(19%)+νNC(10%)+δONO(12%) |
| 92 | 1496 | 1446 | 2.036 | δONO(15%) |
| 93 | 1532 | 1481 | 5.956 | νON(24%)+δONC(18%)+δONO(11%) |
| 94 | 1556 | 1505 | 214.8 | νON(12%)+δONO(12%)+γOCON(16%) |
| 95 | 1557 | 1506 | 114.8 | δONC(18%) |
| 96 | 1574 | 1522 | 28.68 | τHCCC(15%) |
| 98 | 1609 | 1556 | 184.7 | νCC(10%) |

**Table 4.** (Continued).

| Modes | Unscaled | Scaled [a] | IR | Assignment [TED] [b] ≥ 10% |
|---|---|---|---|---|
| 100 | 1628 | 1574 | 233.8 | δHCC(13%) |
| 101 | 1638 | 1574 | 85.83 | δHCC(11%) |
| 102 | 1660 | 1605 | 494.4 | τHCCC(19%) |
| 103 | 1691 | 1635 | 742.0 | νCH(14%)+τHCCC(28%) |
| 104 | 2998 | 2899 | 1022 | τHCNC(31%)+τCOHC(13%) |
| 105 | 3153 | 3049 | 323.3 | τHCNC(12%)+τHCCC(14%) |
| 106 | 3176 | 3071 | 7.722 | νCH(20%)+τHCCC(10%) |
| 107 | 3180 | 3075 | 209.6 | δHCC(23%)+τHCNC(20%)+τHCCC(28%) |
| 108 | 3186 | 3080 | 4.256 | νCH(24%)+τHCCN(22%) |
| 109 | 3198 | 3092 | 0.632 | νCH(51%)+δHCC(10%)+τHCCC(10%) |
| 110 | 3210 | 3105 | 3.884 | δHCC(18%)+δHCN(43%)+τHCCN(11%)+τHCNC(12%) |
| 111 | 3210 | 3105 | 2.035 | δHCC(40%)+τHCCN(11%) |
| 112 | 3224 | 3118 | 1.787 | δHCC(50%)+τHCCC(10%) |
| 113 | 3232 | 3125 | 11.67 | νCH(84%) |
| 114 | 3233 | 3126 | 11.52 | νCH(60%)+τHCCC(13%) |

[a] Wavenumbers are scaled with 0.967 for B3LYP/6-311G(d,p) basis set.
[b] TED: total energy distribution, ν; stretching, δ; in-plane-bending, γ; out-of plane bending, τ;torsion, ρ: rocking, *w*; wagging, t; twisting, sym; symmetric and asym; asymmetric.

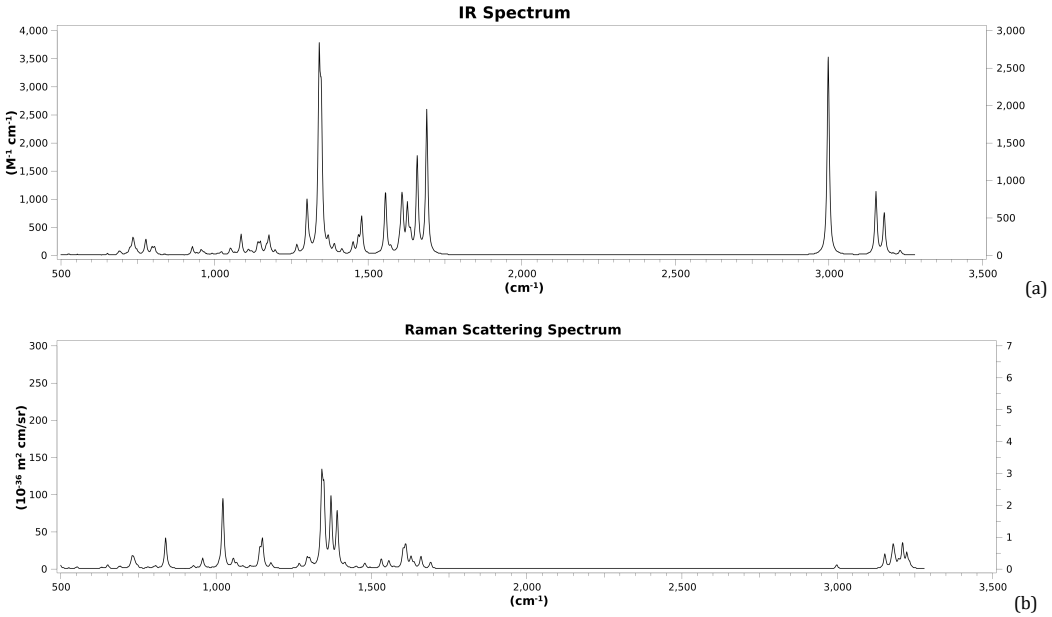


**Figure 7.** Calculated FT-IR (a) and FT-RAMAN (b) spectrums of the title compound, 2-PyrTPPc.

### *3.4. The frontier orbitals analysis*

To understand the stability and reactivity of chemical compounds on a global scale, it is essential to perform a detailed analysis of several key properties. Among these, frontier molecular orbitals (FMO) are vital to elucidate the electronic structure of molecules, as they represent the highest occupied orbitals (HOMO) and lowest unoccupied orbitals (LUMO) involved in chemical bonding and reactions [41]. The energy difference between these orbitals is critical, as it directly influences a compound's reactivity; narrower gaps often correspond to increased reactivity due to the ease of electron excitation [42]. Hardness refers to the resistance of a molecule to deformation and chemical change, while softness indicates a tendency to engage in chemical interactions [43]. These characteristics provide valuable insights into the anticipated behavior of compounds in various chemical environments. Furthermore, the chemical potential is analyzed to understand the likelihood that a compound changes in response to variations in external conditions. This potential illustrates how a substance interacts with its environment, affecting its stability and reactivity. These comprehensive analyzes not only improve our understanding of the intrinsic properties of chemical compounds, but also help predict their behavior in real-world applications and reactions under various conditions [44]. The energy difference between the HOMO-LUMO orbitals and other global reactivates for the title compound was calculated in Table 5. As can be seen from the plot of the HOMO level, all negative regions are spread over the picrate anion of the title molecule. At the LUMO level, the negative regions are spread over the 2-(pyridine-2-ylthio)-pyridine-1-ium moiety. The atomic orbital compositions of the molecular orbitals are shown in Figure 8. The HOMO value is -5.70 eV, while the LUMO value is -3.15 eV, and the ΔE value calculated at the DFT level is 2.55 eV. This small energy value of the title compound explains the high chemical reactivity and the low kinetic stability due to the narrow energy space of electronic transitions [45,46].

### *3.5. Molecular electrostatic potential (MEP) analysis*

MEP is used for prediction by highlighting the areas of nucleophilic and electrophilic attack depending on the electron densities (ED) on the molecule. It also identifies the hydrogen bond interaction sites [47]. The electrophilic and nucleophilic reactivity by the map of MEP are represented as different colors such as blue, green, and yellow or red from positive, neutral to negative regions, respectively. The red and blue colors in the MEP structure indicate more electron-rich regions and less electron-rich regions, respectively [48]. DFT calculations using the optimized structure with the B3LYP/6-311G(d,p) basis set were performed to determine the MEP surface of the title compound.

**Table 5.** Calculated electronic parameters of the title compound, 2-PyrTPPc using the DFT method at the B3LYP/6-311G(d,p) level.

| Parameters | Gas phase |
|---|---|
| Electronic energy (a.u.) | -1814.908 |
| Excitation energy (eV) | 2.065 |
| $E_{HOMO}$ (eV) | -5.70 |
| $E_{LUMO}$ (eV) | -3.15 |
| Energy band gap [$\Delta E = E_{LUMO}$-$E_{HOMO}$] (eV) | 2.55 |
| Ionization energy [I = -$E_{HOMO}$] (eV) | 5.70 |
| Electron affinity [A = -$E_{LUMO}$ ] (eV) | 3.15 |
| Electronegativity [$\chi$ =(I+A)/2 ] (eV) | 4.43 |
| Chemical hardness [$\eta$ =(I-A)/2)] (eV) | 1.28 |
| Chemical softness [$\zeta = 1/2\eta$] ($eV^{-1}$) | 0.78 |
| Chemical potential [$\mu$ = -(I+A)/2] (eV) | -4.43 |
| Electrophilicity index [$\omega = \mu^2/(2\eta)$] (eV) | 7.68 |

**Table 6.** The second-order perturbation energies E(2)(kcal/mol) correspond to the most important charge transfer interaction(donor-acceptor) in 2-PyrTPPc by the DFT/B3LYP/6-311G(d,p) method.

| Donor NBO(i) | Acceptor NBO(j) | E(2)[a] | E(j)-E(i)[b] a.u. | F(i,j)[c] a.u. |
|---|---|---|---|---|
| π(N7 -C21) | LP(1) C22 | 13.46 | 0.27 | 0.069 |
| π(N7 -C21) | π*(C25 -C27) | 19.40 | 0.39 | 0.079 |
| π(N12 -C20) | π*(C23 -C29) | 11.03 | 0.34 | 0.056 |
| | π*(C24 -C28) | 25.77 | 0.32 | 0.084 |
| σ(C20 -H35) | σ*(N12 -C24) | 5.85 | 1.04 | 0.070 |
| σ(C22 -H33) | σ*(N7 -C21) | 5.68 | 0.95 | 0.066 |
| π(C23 -C29) | π*(N12 -C20) | 35.19 | 0.24 | 0.084 |
| | π*(C24 -C28) | 20.28 | 0.26 | 0.065 |
| π(C24 -C28) | π*(N12 -C20) | 17.25 | 0.26 | 0.061 |
| | π*(C23 -C29) | 21.75 | 0.30 | 0.073 |
| π(C25 -C27) | LP*(1) C26 | 45.02 | 0.18 | 0.094 |
| | π*(N7 -C21) | 14.17 | 0.21 | 0.053 |
| σ(C28 -H37) | σ*(N12 -C24) | 5.25 | 1.04 | 0.066 |
| LP(1) S1 | σ*(N7 -C21) | 5.18 | 1.07 | 0.067 |
| LP(2) S1 | π*(N7 -C21) | 35.21 | 0.18 | 0.078 |
| | π*(C24 -C28) | 19.21 | 0.25 | 0.063 |
| LP(1) N12 | σ*(N7 -H40) | 25.07 | 0.75 | 0.124 |
| | σ*(C20 -C23) | 7.76 | 0.93 | 0.078 |
| | σ*(C24 -C28) | 9.43 | 0.90 | 0.085 |
| LP(1) C22 | π*(N7 -C21) | 432.40 | 0.03 | 0.124 |
| LP*(1) C26 | π*(C25 -C27) | 61.28 | 0.11 | 0.101 |
| π*(N7 -C21) | π*(C25 -C27) | 31.87 | 0.08 | 0.069 |
| π*(N12 -C20) | π*(C23 -C29) | 103.18 | 0.04 | 0.088 |
| | π*(C24 -C28) | 159.65 | 0.02 | 0.076 |
| π*(C24 -C28) | π*(C23 -C29) | 178.71 | 0.02 | 0.084 |

[a] E(2) means the energy of hyperconjugative interactions.
[b] Energy difference between donor and acceptor i and j NBO orbitals.
[c] F(i,j) is the Fock matrix element between the i and j NBO orbitals.

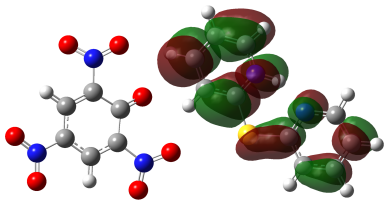

$E_{LUMO}$ = - 3.15 eV

$\Delta E$ = 2.55 eV

$E_{HOMO}$ = - 5.70 eV

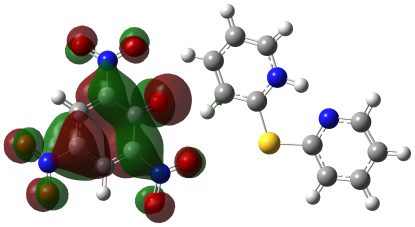

**Figure 8.** Frontier molecular orbitals (HOMO and LUMO) diagram for the title compound, 2-PyrTPPc.

Figure 9 shows the mapped MEP surface of the investigated compound. The color code of the title compound is in the range of -8.765e$^{-2}$ to 8.765e$^{-2}$. In the MEP mapping, the picrate anion moiety with three nitro groups is highlighted in red, while the 2-(pyridine-2-ylthio)pyridine-1-ium moiety is highlighted in blue. Therefore, it can be seen from Figure 9 that the anionic moiety is the electronegative region, while the cationic moiety is the electropositive region.

**Table 7.** Calculated thermodynamic parameters of the title compound

| Parameters | B3LYP/6-311G(d,p) |
|---|---|
| Temperature (K) | 298.15 |
| Pressure (atm) | 1 |
| The sum of electronic and zero-point Energies (a.u.) | -1814.636376 |
| Zero-point vibrational energy (kcal/mol) | 170.16634 |
| Rotational constants (GHz) | 0.29215 |
| | 0.06797 |
| | 0.05720 |
| E (Thermal) (KCal/Mol) | 186.008 |
| Specific heat ($C_v$) (cal /mol K) | 91.777 |
| Entropy (S) (cal/mol K) | 183.977 |
| Dipole moment (Debye) | 24.6258 |

**Table 8.** The thermodynamic properties of the title compound, 2-PyrTPPc at different temperatures at B3LYP/6-311G(d,p) level.

| T (K) | $C°_{p,m}$ (cal/mol.K) | $S°_m$ (cal/mol.K) | $\Delta H°$ (kcal/mol) |
|---|---|---|---|
| 100 | 182.981 | 476.807 | 11.903 |
| 200 | 287.291 | 635.564 | 35.403 |
| 298.15 | 392.310 | 769.872 | 68.761 |
| 300 | 394.257 | 772.305 | 69.489 |
| 400 | 493.125 | 899.605 | 113.976 |
| 500 | 575.378 | 1018.809 | 167.550 |
| 600 | 640.781 | 1129.730 | 228.487 |
| 700 | 692.455 | 1232.541 | 295.248 |
| 800 | 733.703 | 1327.798 | 366.631 |
| 900 | 767.108 | 1416.211 | 441.728 |
| 1000 | 794.535 | 1498.499 | 519.854 |

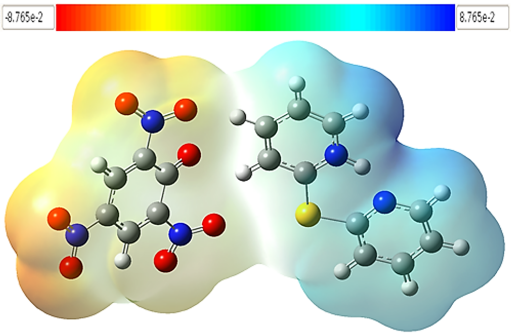


**Figure 9.** Molecular electrostatic potential map calculated at B3LYP/6-311G(d,p) level for the title compound, 2-PyrTPPc.

### *3.6. Natural bond orbital (NBO) analysis*

NBO analysis provides sufficient fundamentals for the investigation of charge transfer or conjugative interactions in molecular systems and also provides abundant methods for studying intramolecular and intermolecular bonding and interaction among bonds [49]. The interacting stabilization energy, some electron donor orbital and acceptor orbital disturbance theory are declared [50,51]. The E(2) value exhibits the interaction energy between the electron acceptor and the electron donors, and this value is greater than the dependence of the electron donation from the donor to the acceptor. The delocalization of electron density between occupied Lewis type (bond or lone pair) NBO orbitals and formally unoccupied (antibonding or Rydberg) non-Lewis NBO orbitals corresponds to a stabling donor-acceptor interaction [52]. Table 6 displays the most potent interactions and electron delocalization values. This information is critical in understanding the underlying chemical mechanisms and can significantly enhance our ability to predict molecular behavior with greater accuracy.

### *3.7. Thermal analysis*

The TG curve of the title compound is shown in Figure 10. Important information about thermal stability, compound decomposition, and crystal purity can be obtained by thermogravimetry and differential thermogravimetry (TG/DTG) [53]. From the TG curve, it is clear that there is no weight loss between 30 and 157 °C and shows that the title compound is stable up to 157.46 °C and moisture-free. Furthermore, the crystal has a one-step decomposition. After 157.46 °C, there is no residue left due to decomposition resulting in the release of volatile substances such as $CH_4$, $NO_2$, $NH_3$, CO, $CO_2$ and $H_2S$ molecules [54]. The purity of the title compound crystal is also illustrated by the sharpness of the thermogram.

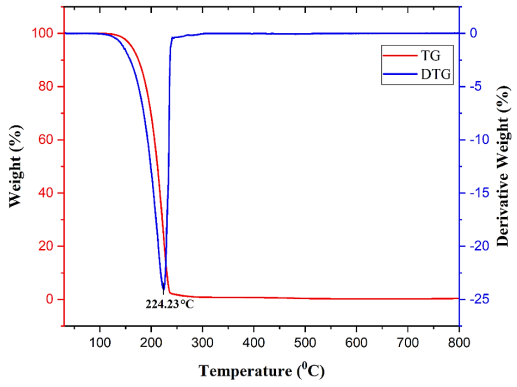


**Figure 10.** TG/DTG thermograms of the title compound, 2-PyrTPPc.

### *3.8. Thermodynamic properties*

Statistically thermodynamic parameters such as specific heat capacity (Cp), enthalpy (H), entropy (S), zero-point

vibration energy (ZPVE), rotation constants, and rotational temperature thermodynamic parameters were calculated using the B3LYP/6-311G(d,p) method in the ground state (Table 7).

The determination of thermochemical parameters such as the standard heat capacity of constant pressure (Cp), enthalpy (H) and entropy (S) and identification of the behavior of chemical compounds under temperature is quite important [55]. Properties of interest exert a direct influence on the vibrational dynamics between the atoms within chemical compounds. Furthermore, they play a crucial role in the assessment of the energy and heat associated with both chemical reactions and physical transformations, as outlined in Table 8.

## 4. Conclusions

Using a different route, we synthesized a new picrate salt. FT-IR, $^{1}$H NMR, and $^{13}$C NMR spectral techniques were used to characterize the molecular structure of the title compound. The single crystals were deliberately grown using a meticulous slow evaporation method with tetrahydrofuran as a solvent. The molecular form was determined conclusively by rigorous X-ray structure analysis, enabling the precise calculation of geometrical parameters. In general, while the formation of the picrate salt of the aromatic amine is expected, the formation of the picrate salt of the amine synthesized through the reactions of substituted benzyne(pyridyne)-type intermediates is assumed according to the spectral data. Experimental data such as X-ray, FTIR, and Raman with optimized geometric parameters, and the vibrational frequency data obtained as the theoretical calculations have been tested using the B3LYP/6-311G (d, p) basis set. Furthermore, using these data, the analysis of HOMO and LUMO energy, electronegativity (χ), hardness (η), softness (S), MEP and NBO of the picrate compound were also calculated. The properties of interest directly affect the vibrational dynamics of atoms within chemical compounds. These measurements are essential for evaluating energy transfer and thermal changes during chemical reactions and physical transformations. A thorough analysis of these processes provides valuable insights into the interactions among substances, such as the mechanisms by which energy is absorbed or released. TG-DTG analysis demonstrated the thermal stability of the 2-PyrTPPc crystal and indicated its good crystallinity with single-stage decomposition.

## Acknowledgements

We are also grateful to TUBITAK ULAKBIM, the High Performance and Grid Computing Center (TRUBA Resources).

## CRediT authorship contribution statement

Conceptualization: Fatma Aydin; Methodology: Fatma Aydin; Software: Asli Ozturk Kiraz; Validation: Fatma Aydin, Asli Ozturk Kiraz; Formal Analysis: Asli Ozturk Kiraz; Investigation: Fatma Aydin; Resources: Fatma Aydin; Data Curation: Fatma Aydin, Asli Ozturk Kiraz; Writing-Original Draft: Fatma Aydin, Asli Ozturk Kiraz; Writing-Review And Editing: Fatma Aydin, Asli Ozturk Kiraz; Visualization: Fatma Aydin, Asli Ozturk Kiraz; Funding Acquisition: Fatma Aydin, Asli Ozturk Kiraz; Project Administration: Fatma Aydin.

## Disclosure statement

Conflict of interest: The authors declare no financial interest/personal relationships which may be considered as potential competing interests.
Ethical approval: All ethical guidelines have been adhered.
Sample availability: Samples of the compounds are available from the author.

## Supporting information

CCDC-2335699 contains the supplementary crystallographic data for the structure reported in this article. These data can be obtained free of charge via http://www.ccdc.cam.ac.uk/data_request/cif, by e-mailing data_request@ccdc.cam.ac.uk or by contacting The Cambridge Crystallographic Data Centre, 12, Union Road, Cambridge CB2 1EZ, UK; fax:+44-1223-336033.

## Funding

This work was financially supported by the Çanakkale Onsekiz Mart University (Grant Number: FBA-2016-672) and Pamukkale University (Grant numbers: 2018FEBE002 and 2020FEBE012).

## ORCID and Email

Fatma Aydin
faydin@comu.edu.tr
https://orcid.org/0000-0002-7219-6407
Asli Ozturk Kiraz
aslio@pau.edu.tr
https://orcid.org/0000-0001-9837-0779

## References

[1]. Moran, D.; Sukcharoenphon, K.; Puchta, R.; Schaefer, H. F.; Schleyer, P. v.; Hoff, C. D. 2-Pyridinethiol/2-Pyridinethione Tautomeric Equilibrium. A Comparative Experimental and Computational Study. *J. Org. Chem.* **2002**, *67* (25), 9061–9069.
[2]. Jones, R. A.; Katritzky, A. R. 721. Tautomeric pyridines. Part I. Pyrid-2- and -4-thione. *J. Chem. Soc.* **1958**, 3610.
[3]. Barton, D. H.; Hesse, R. H.; O'Sullivan, A. C.; Pechet, M. M. A new procedure for the conversion of thiols into reactive sulfenylating agents. *J. Org. Chem.* **1991**, *56* (23), 6697–6702.
[4]. Hoogerheide, J.; Scott, R. Use of 2-mercaptopyridine for the determination of alkylating agents in complex matrices: application to dimethyl sulfate. *Talanta* **2005**, *65* (2), 453–460.
[5]. De C.T. Carrondo, M.; Dias, A.; Garcia, M. H.; Mirpuri, A.; Fátima, M.; Piedade, M.; Salema, M. S. Mercaptopyridine complexes of dicyclopentadienylmolybdenum and -tungsten: Preparation and electrochemistry. The structure of [Mo(η5-C5H5)2(2-SNC5H4)][PF6]. *Polyhedron* **1989**, *8* (20), 2439–2447.
[6]. Yoon, S. A.; Kim, W.; Sharma, A.; Verwilst, P.; Won, M.; Lee, M. H. A Fluorescent Cy7-Mercaptopyridine for the Selective Detection of Glutathione over Homocysteine and Cysteine. *Sensors* **2018**, *18* (9), 2897.
[7]. Maruyama, K.; Nagasawa, H.; Suzuki, A. 2,2′-Bispyridyl disulfide rapidly induces intramolecular disulfide bonds in peptides. *Peptides* **1999**, *20* (7), 881–884.
[8]. Suguna, S.; Subbareddy, Y.; Jose, T. J.; Chand, N. R.; Ramakrishna, D.; Praveen, P. L. Synthesis, growth, and optical applications of N, N′-bis (2-aminophenyl) ethane-1,2-diammonium picrate: An organic crystal. *J. Mol. Struct.* **2024**, *1300*, 137295.
[9]. Kolandaivelu, S.; Rajamoni, J.; Kandasamy, S. N-H…O, C-H… O hydrogen-bonded supramolecular frameworks in 4-fluoroanilinium and dicyclohexylaminium picrate salts. *Struct Chem* **2019**, *31* (3), 899–908.
[10]. Ramarajan, D.; Tamilarasan, K.; Milenković, D.; Marković, Z.; Sudha, S.; Subhapriya, P. Experimental and theoretical investigations of an organic nonlinear optical material p-toluidinium picrate – A comparative study. *J. Mol. Struct.* **2019**, *1195*, 73–84.
[11]. Arslan, N. B.; Aydin, F. The crystal magnification, characterization, X-ray single crystal structure, thermal behavior, and computational studies of the 2,4,6-trimethylpyridinium picrate. *Eur. J. Chem.* **2022**, *13* (4), 468–477.
[12]. Aydin, F.; Arslan, N. B. Synthesis and structural characterization and DFT calculations of the organic salt crystal obtaining 9-aminoacridine and picric acid: 9-Aminoacridinium picrate. *Eur. J. Chem.* **2023**, *14* (3), 376–384.
[13]. Karthigha, S.; Krishnamoorthi, C. Synthesis, growth, crystal structure, optical and third order nonlinear optical properties of quinolinium derivative single crystal: PNQI. *J. Phys. Chem. Solids* **2018**, *114*, 133–140.
[14]. Chandramohan, A.; Bharathikannan, R.; Kandavelu, V.; Chandrasekaran, J.; Kandhaswamy, M. Synthesis, crystal growth, structural, thermal and optical properties of naphthalene picrate an organic NLO material. *Spectrochim. Acta A: Mol. Biomol. Spectrosc.* **2008**, *71* (3), 755–759.
[15]. Bozkuş, S. I.; Hope, K. S.; Yüksel, B.; Atçeken, N.; Nazır, H.; Atakol, O.; Şen, N. Characterization and properties of a novel energetic Co-crystal formed between 2,4,6-Trinitrophenol and 9-Bromoanthracene. *J. Mol. Struct.* **2019**, *1192*, 145–153.
[16]. Ghazaryan, V.; Fleck, M.; Petrosyan, A. Structure and vibrational spectra of l-alanine l-alaninium picrate monohydrate. *J. Mol. Struct.* **2012**, *1015*, 51–55.

[17]. Fleck, M.; Ghazaryan, V.; Petrosyan, A. β-Alaninium picrate: A new salt with di-β-alaninium dimeric cation. *J. Mol. Struct.* **2012**, *1019*, 91–96.
[18]. Ghazaryan, V.; Zakharov, B.; Boldyreva, E.; Petrosyan, A. l-Methioninium picrate. *Spectrochim. Acta A: Mol. Biomol. Spectrosc.* **2015**, *142*, 344–349.
[19]. Suguna, S.; Anbuselvi, D.; Jayaraman, D.; Nagaraja, K.; Jeyaraj, B. Synthesis, growth, structural and optical studies of organic nonlinear optical material – Piperazine-1,4-diium bis 2,4,6-trinitrophenolate. *Spectrochim. Acta A: Mol. Biomol. Spectrosc.* **2014**, *132*, 330–338.
[20]. Alexandar, A.; Surendran, P.; Sakthy Priya, S.; Lakshmanan, A.; Rameshkumar, P. Growth and characterizations of L-methioninium picrate single crystal for nonlinear optical applications. *J. Nonlinear Optic. Phys. Mat.* **2016**, *25* (04), 1650052.
[21]. Levine, R.; Leake, W. W. Rearrangement in the Reaction of 3-Bromopyridine with Sodium Amide and Sodioacetophenone. *Science* **1955**, *121* (3152), 780–780.
[22]. Puleo, T. R.; Bandar, J. S. Base-catalyzed aryl halide isomerization enables the 4-selective substitution of 3-bromopyridines. *Chem. Sci.* **2020**, *11* (38), 10517–10522.
[23]. Janczak, J. Structure, vibrational characterization and DFT calculations of 1-(diaminomethylene)thiouron-1-ium 2,3-pyridinedicarboxylate. *Struct Chem* **2023**, *35* (4), 1183–1198.
[24]. Kannan, V.; Santha, A.; Sugumar, P.; Brahadeeswaran, S. Investigations on thermal, dielectric, and quantum chemical calculations of 2-amino-5-chloropyridinium 4-aminobenzoate: a nonlinear optical material. *Struct Chem* **2023**, *35* (3), 977–991. https://doi.org/10.1007/s11224-023-02232-x
[25]. Sheldrick, G. M. SHELXS-97 and SHELXL-97 Program for Crystal Structure Solution and Refinement. University of Gottingen, Germany, Germany, 1997.
[26]. Frisch, M. J.; Trucks, G. W.; Schlegel, H. B.; Scuseria, G. E.; Robb, M. A.; Cheeseman, J. R.; Montgomery, J. A.; Vreven, T.; Kudin, K. N.; Burant, J. C.; Millam, J. M.; Iyengar, S. S.; Tomasi, J.; Barone, V.; Mennucci, B.; Cossi, M.; Scalmani, G.; Rega, N.; Petersson, G. A.; Nakatsuji, H.; Hada, M.; Ehara, M.; Toyota, K.; Fukuda, R.; Hasegawa, J.; Ishida, M.; Nakajima, T.; Honda, Y.; Kitao, O.; Nakai, H.; Klene, M.; Li, X.; Knox, J. E.; Hratchian, H. P.; Cross, J. B.; Adamo, C.; Jaramillo, J.; Gomperts, R.; Stratmann, R. E.; Yazyev, O.; Austin, A. J.; Cammi, R.; Pomelli, C.; Ochterski, J. W.; Ayala, P. Y.; Morokuma, K.; Voth, G. A.; Salvador, P.; Dannenberg, J. J.; Zakrzewski, V. G.; Dapprich, S.; Daniels, A. D.; Strain, M. C.; Farkas, O.; Malick, D. K.; Rabuck, A. D.; Raghavachari, K; Foresman, J. B.; Ortiz, J. V.; Cui, Q.; Baboul, A. G.; Clifford, S.; Cioslowski, J.; Stefanov, B. B.; Liu, G.; Liashenko, A.; Piskorz, P.; Komaromi, I.; Martin, R. L.; Fox, D. J.; Keith, T.; Al-Laham, M. A.; Peng, C. Y.; Nanayakkara, A.; Challacombe, M.; Gill, P. M. W.; Johnson, B.; Chen, W.; Wong, M. W.; Gonzalez, C.; Pople, J. A. Gaussian, Inc., Wallingford CT, 2004.
[27]. Dennington, R.; Keith, T. A.; Millam, J. M. GaussView, Version 6, Semichem Inc.; Shawnee Mission, KS, 2016.
[28]. Foresman, J. B.; Frisch, Æ. In Exploring Chemistry with Electronic Structure Methods, 2nd ed.; Gaussian Inc.: Pittsburgh, PA, 1996.
[29]. Walters, P.; Stahl, M. Babel,Vversion 1.1. Department of Chemistry, University of Arizona, Tucson, AZ 85721, 1994.
[30]. Essayem, N.; Lorentz, C.; Tuel, A.; Tâarit, Y. B. 1H NMR evidence for the bi-pyridinium nature of the pyridine salt of H3PW12O40. *Catal. Commun.* **2005**, *6* (8), 539–541.
[31]. Cremer, D.; Pople, J. A. General definition of ring puckering coordinates. *J. Am. Chem. Soc.* **1975**, *97* (6), 1354–1358.
[32]. Burnett, M. N.; Johnson, C. K. (1996). ORTEPIII. Report ORNL-6895. Oak Ridge National Laboratory, Tennessee, USA.
[33]. Steiner, T. The Hydrogen Bond in the Solid State. *Angew. Chem. Int. Ed.* **2002**, *41* (1), 48–76.
[34]. Cook, D. Vibrational spectra of pyridinium salts. *Can. J. Chem.* **1961**, *39* (10), 2009–2024.
[35]. Bryndal, I.; Drozd, M.; Lis, T.; Zaręba, J. K.; Ratajczak, H. Structural diversity of hydrogen-bonded complexes comprising phenol-based and pyridine-based components: NLO properties and crystallographic and spectroscopic studies. *CrystEngComm* **2020**, *22* (27), 4552–4565.
[36]. Moura, A. L.; Machado, P. H.; Corrêa, R. S. Picrate salts with bipyridine derivatives: intramolecular and intermolecular aspects. *Struct Chem* **2023**, *34* (5), 1817–1826.
[37]. Cao, H.; Ben, T.; Su, Z.; Zhang, M.; Kan, Y.; Yan, X.; Zhang, W.; Wei, Y. Absolute Configuration Determination of a New Chiral Rigid Bisetherketone Macrocycle Containing Binaphthyl and Thioether Moieties by Vibrational Circular Dichroism. *Macro Chemistry & Physics* **2005**, *206* (11), 1140–1145.
[38]. Socrates, G. Infrared and Raman Characteristic Group Frequencies: Tables and Charts, 3rd Edition, John Wiley & Sons, Inc., New York 2004.
[39]. Gümüs, H. P.; Tamer, O.; Avci, D.; Tarcan, E.; Atalay, Y. Theoretical investigations on nonlinear optical and spectroscopic properties of 6-(3,3,4,4,4-pentafluoro-2-hydroxy-1-butenyl)-2,4-pyrimidinedione: An efficient NLO material. *Russ. J. Phys. Chem.* **2014**, *88* (13), 2348–2358.
[40]. Zhang, J.; Li, T.; Liang, J.; Chen, L.; Zeng, Y.; Yang, L.; Zhou, J.; Ni, C. Synthesis, crystal structure, vibrational spectra, optical properties of disubstituted benzyl triphenylphosphinium picrate: Experiment and DFT/TDDFT calculations. *J. Mol. Struct.* **2020**, *1210*, 127972.
[41]. Parr, R. G.; Pearson, R. G. Absolute hardness: companion parameter to absolute electronegativity. *J. Am. Chem. Soc.* **1983**, *105* (26), 7512–7516.
[42]. Xavier, S.; Periandy, S.; Ramalingam, S. NBO, conformational, NLO, HOMO–LUMO, NMR and electronic spectral study on 1-phenyl-1-propanol by quantum computational methods. *Spectrochim. Acta A: Mol. Biomol. Spectrosc.* **2015**, *137*, 306–320.
[43]. Chattaraj, P. K.; Sarkar, U.; Roy, D. R. Electrophilicity Index. *Chem. Rev.* **2006**, *106* (6), 2065–2091.
[44]. Parr, R. G.; Szentpály, L. v.; Liu, S. Electrophilicity Index. *J. Am. Chem. Soc.* **1999**, *121* (9), 1922–1924.
[45]. Miar, M.; Shiroudi, A.; Pourshamsian, K.; Oliaey, A. R.; Hatamjafari, F. Theoretical investigations on the HOMO–LUMO gap and global reactivity descriptor studies, natural bond orbital, and nucleus-independent chemical shifts analyses of 3-phenylbenzo[*d*]thiazole-2(3*H*)-imine and its *para*-substituted derivatives: Solvent and substituent effects. *J. Chem. Res.* **2020**, *45* (1-2), 147–158.
[46]. Kayalvizhi, K.; Balakrishnan, C.; Suppuraj, P.; Lakshmanan, P.; Kalpana, S.; Senthan, S. Synthesis, structural characterization, Hirshfeld surface and theoretical studies of 2-bromopyridinium picrate. *Mol. Cryst. Liq. Cryst.* **2023**, *760* (1), 85–98.
[47]. Politzer, P.; Murray, J. S. The fundamental nature and role of the electrostatic potential in atoms and molecules. *Theor. Chem. Acc.: Theory Comput. Model. (Theor. Chim. Acta)* **2002**, *108* (3), 134–142.
[48]. Geerlings, P.; Proft, F. D.; Ayers, P. Chapter 1 Chemical reactivity and the shape function. *Theor. Comput. Chem.* **2007**, *19*, 1–17.
[49]. Snehalatha, M.; Ravikumar, C.; Hubert Joe, I.; Sekar, N.; Jayakumar, V. Spectroscopic analysis and DFT calculations of a food additive Carmoisine. *Spectrochim. Acta A: Mol. Biomol. Spectrosc.* **2009**, *72* (3), 654–662.
[50]. James, C.; Raj, A. A.; Reghunathan, R.; Jayakumar, V. S.; Joe, I. H. Structural conformation and vibrational spectroscopic studies of 2,6-bis(*p*-*N*,*N*-dimethyl benzylidene)cyclohexanone using density functional theory. *J. Raman Spectroscopy* **2006**, *37* (12), 1381–1392.
[51]. Liu, J.; Chen, Z.; Yuan, S. Study on the prediction of visible absorption maxima of azobenzene compounds. *J. Zheijang Univ Sci B.* **2005**, *6* (6), 584–589.
[52]. Sebastian, S.; Sundaraganesan, N. The spectroscopic (FT-IR, FT-IR gas phase, FT-Raman and UV) and NBO analysis of 4-Hydroxypiperidine by density functional method. *Spectrochim. Acta A: Mol. Biomol. Spectrosc.* **2010**, *75* (3), 941–952.
[53]. Coats, A. W.; Redfern, J. P. Thermogravimetric analysis. A review. *Analyst* **1963**, *88* (1053), 906.
[54]. Jauhar, R. M.; Viswanathan, V.; Vivek, P.; Vinitha, G.; Velmurugan, D.; Murugakoothan, P. A new organic NLO material isonicotinamidium picrate (ISPA): crystal structure, structural modeling and its physico-chemical properties. *RSC. Adv.* **2016**, *6* (63), 57977–57985.
[55]. Ott, J. B.; Boerio-Goates, J.; Beasley, D. *Chemical Thermodynamics: Principles and Applications. Appl. Mech. Rev.* **2001**, *54* (6), B110–B110.